2014 American Control Conference (ACC)
June 4-6, 2014. Portland, Oregon, USA

On time-optimal anti-sway controller design for bridge cranes

Michele Ermidoro, Simone Formentin, Alberto Cologni, Fabio Previdi and Sergio M. Savaresi

Abstract— **In this paper, we analyze and discuss the time optimal control problem for bridge cranes. Specifically, we employ the geometric approach introduced in [12] to address the control issue without computing the analytic trajectory of the costate. As a second contribution, we show that an alternative approach based on a proportional controller accounting for the limits of the control action can be tuned to resemble to the time-optimal solution, but with simpler and more robust implementation. The above ideas are validated by means of some simulation examples.**

I. INTRODUCTION

An overhead bridge crane is a crane typically used for challenging manipulation tasks in many industrial applications, *e.g* in the refinement of steel or to handle raw materials in the automobile industry. It consists of parallel runways with a traveling bridge spanning the gap. A trolley, the lifting component of a crane, can travel along the bridge.

In many cases, the cost of a bridge crane can be largely offset with savings from not renting mobile cranes when heavy process equipment is used. Unfortunately, modern crane systems offer accurate positioning but are also usually characterized by a poor damping of the load swinging. This problem has a detrimental effect on the maneuvering performance and, more worrisome, on the safety of human operators. Some solutions to deal with such a problem have been presented in, *e.g.*, [15], [8], [13], [6].

In this paper, we will focus on the most critical phenomenon for crane/human interaction: the residual load swinging when the bridge crane stops. Specifically, as far as we are aware, we will address the problem from a novel perspective, *i.e.* our aim will be to find a simple control law which *minimizes the time needed to stop*.

Since the 1960s, it is well known that time-optimal control design for real-world systems (for which the inputs are bounded) can be dealt using open-loop approaches like the input shaper in [14] or closed-loop strategies like bang-bang control laws [7]. However, current feedback loops are not easy to implement as the practical derivation of the number of switches and the switching times is all but straightforward, mainly because the costate trajectory is hard to compute [11].

Nonetheless, in this work, we will show that the time-optimal control problem of the overhead bridge crane can be reformulated according to the recent study in [12], where a geometric approach can be used to compute the required quantities, instead of deriving the analytic trajectory of the costate vector. More specifically, in [12], it is shown that, for second-order systems like the bridge crane considered herein, the switching curve and the boundaries between regions of constant control can be transformed into collections of logarithmic spirals. The number of switches and the switching times can then be geometrically determined by only employing such diagrams. This will be done in a simulation environment, where the bridge crane will show good nominal performance.

Unfortunately, the performance of the above time-optimal strategy is strongly related to the model accuracy. This fact may represent a problem as the weight of the load, the length of the rope and especially the damping coefficients may vary a lot along different operating conditions. Therefore, as a second contribution, we show that we can approximate the time-optimal controller with a suitably tuned proportional controller, which is less dependent on the parametric ucertainty and easier to implement in a real-world bridge crane. Simple LMI conditions can be employed to verify the internal stability of the closed-loop system with the proportional controller in the loop in the actual case where the input speed is bounded (see, *e.g.* [3], [4], [2]). In a simulation environment, the proposed proportional controller will in fact prove to be approximately as effective as the time-optimal one, but more robust.

The remainder of the paper is as follows. In Section II, the bridge crane system and the model considered for controller design will be defined and described in detail. The time-optimal control strategy and its approximation using proportional control design are presented in Section III, where the LMI method to verify that the closed-loop system is internally stable is also illustrated. The performance of the above approaches will be assessed on a simulator of the bridge crane in Section IV. The paper is ended by some concluding remarks.

II. THE BRIDGE-CRANE MODEL

The typical setup of a bridge crane is illustrated in Figure1, where the two main components of the system are shown: the bridge, which moves along the Y axis on the track, and the trolley, which moves along the X axis on the bridge. The load is connected to the trolley by a rope and can oscillate along any direction.

The system is considered completely decoupled as often done in the literature (see *e.g.* [10]), thus the system can be reduced, for each axis, to a mono-axial cart-pendulum of the type illustrated in Figure 2. The notation is as follows: $x_M(t)$, $\dot{x}_M(t)$, $\ddot{x}_M(t)$ denote, respectively, the position, the

M. Ermidoro, S. Formentin, A. Cologni and F. Previdi are with the Dipartimento di Ingegneria, Università degli Studi di Bergamo, via Marconi 5, 24044 Dalmine (BG), Italy. S.M. Savaresi is with the Dipartimento di Elettronica e Informazione, Politecnico di Milano, Piazza L. Da Vinci 32, 20133 Milano, Italy. Email: michele.ermidoro@unibg.it

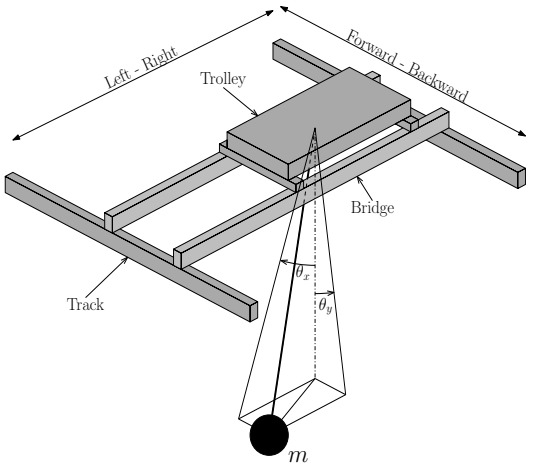

Fig. 1. The typical structure of a bi-dimensional bridge crane. The trolley moves right or left (X axis) on the bridge, which moves forward or backward (Y axis) on the track. The payload is connected to the trolley using a rigid rope and it can swing on both axes.

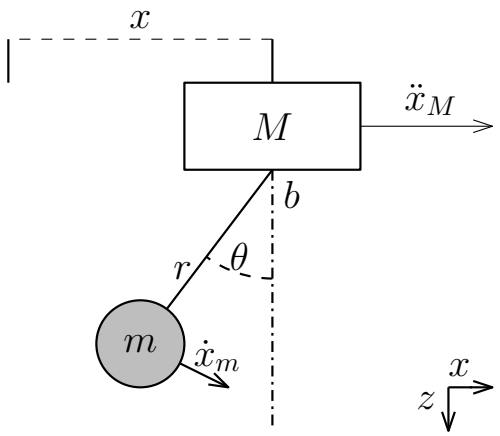

Fig. 2. Structure of a mono-dimensional bridge crane.

speed and the acceleration of the trolley, while M is the mass of the trolley; analogously, $x_m(t)$, $\dot{x}_m(t)$, $\ddot{x}_m(t)$ denote, respectively, the position, the speed and the acceleration of the payload and m is the mass of the payload. The other quantities are r, which indicates the length of the rope, b, that is the viscous friction coefficient, and $\theta(t)$, which models the oscillation angle.

In order to make the model simple enough for control design, the following assumptions will be made.

- The payload is connected to the trolley by a massless, rigid rope.
- The trolley and the bridge move along the track without slipping.
- Each motor is regulated by means of an inner speed control loop, which is assumed to be ideal. In other words, for each time instant, the reference speed is supposed to be equal to the actual one. The speed of the trolley then becomes the input variable for bridge crane control.
- The moment of inertia of the load is neglected, and the load itself is treated as a point mass (notice that this approximation is valid also in case of a multi-wire rope [5]).
- The speed of the motors is bounded.

The model can be deduced using the Eulero-Lagrange equations of motion:

$$\frac{d}{dt}\frac{\delta L}{\delta \dot{q}_k} - \frac{\delta L}{\delta q_k} = \tau_k \quad ; \quad k = 1...n \tag{1}$$

where $L = T - V$ is the Lagrangian of the system, defined as the difference between the kinetic and the potential energy, n is the number of degrees of freedom (DOF) of the system, $\{q_1...q_n\}$ are a set of generalized coordinates and $\{\tau_1...\tau_n\}$ represents a set of generalized force associated to the coordinates. In bridge cranes, the position is controlled by the operator, so we consider $q = \theta$. The only external force related to the oscillation angle is the viscous friction, so $\tau = b\dot{\theta}$ where b is the friction coefficient. Solving (1), the equation of motion

$$\ddot{\theta}(t) = -\frac{1}{r}\left(\ddot{X}(t)\cos\theta(t) + g\sin\theta(t) - \frac{b}{mr}\dot{\theta}(t)\right) \tag{2}$$

is obtained. Linearizing the system about $\dot{\theta} = 0$, $\theta = 0$ and $u = 0$, considering that the real input is the speed of the trolley, we have to consider

$$F(s) = \frac{\theta(s)}{\dot{X}(s)} = \frac{-\frac{1}{r}s}{s^2 + \frac{b}{mr^2}s + \frac{g}{r}} \tag{3}$$

By writing the system in the observable canonical form and recalling that the input is saturated, the final model can be rewritten, in its state-space form, as:

$$\begin{gathered} \dot{x} = Ax + B\sigma(u) \\ A = \begin{bmatrix} 0 & 1 \\ -\frac{g}{r} & -\frac{b}{mr^2} \end{bmatrix},\ B = \begin{bmatrix} -\frac{1}{r} \\ -\frac{b}{mr^3} \end{bmatrix}, \end{gathered} \tag{4}$$

where $\sigma(u) = \max(\min(u_{max}, u), u_{min})$ and u_{min}, u_{max} denote the lower and upper limits of u, respectively.

Moreover, from now on, we define the state vector as $x = [x_1, x_2]^T = [\theta, \dot{\theta}]^T$ and the initial and final conditions will be of the form $x_0 = [\theta_0, 0]^T$ and $x_r = [0, 0]^T$.

III. Time-optimal anti-sway controller design

In this section, the time-optimal control strategy introduced in [12] is briefly recalled and rewritten in order to be directly applied to the bridge crane control problem. A proportional control design approach with stability check will be then presented as a way to approximate the time-optimal control action. The performance and effectiveness of the above approaches will be instead shown in the next section.

A. Time-Optimal control

In the bridge crane application, the performance index to minimize is the time to stop the payload (*i.e.*, to move it from the initial condition x_0 to the final condition x_r). Formally, the cost function is

$$J = \int_0^t dt. \tag{5}$$

which must be evaluated under the dynamical constraints (4).

The standard approach to a time-optimal control problem with bounded input involves the application of the Pontryagin Minimum Principle (PMP) [11], yielding the bang-bang law:

$$u^*(t) = \begin{cases} u_{min}, & if\ \psi^T(t)\,B < 0, \\ u_{max}, & if\ \psi^T(t)\,B > 0 \end{cases} \tag{6}$$

where $\psi(t)$ is the costate vector.

To solve the time-optimal control problem, the approach in [12] avoids the calculation of the evolution of costate, by introducing a geometric solution for the computation of the switching times. Next, we briefly recall the main passages of such an approach.

Firstly, consider the generic second order system of the form

$$\frac{Y(s)}{U(s)} = \frac{b_1 s + b2}{s^2 + a_1 s + a2} \tag{7}$$

By comparing it with (3), the correspondance between the parameters turns out to be

$$\begin{aligned} a_1 &= \frac{b}{mr^2} \quad , a_2 = \frac{g}{r} \\ b_1 &= -\frac{1}{r} \quad , b_2 = 0. \end{aligned} \tag{8}$$

Consider now the affine mapping of the state of the system:

$$\begin{aligned} &M^-_{\substack{min,\\ max}} : \mathbb{R}^2 \to \mathbb{R}^2 \\ &\begin{bmatrix} x_1 \\ x_2 \end{bmatrix} \mapsto \begin{bmatrix} X \\ Y \end{bmatrix} = A^{-1}_{\substack{min,\\ max}} \left(\begin{bmatrix} x_1 \\ x_2 \end{bmatrix} - B_{\substack{min,\\ max}} \right) \end{aligned} \tag{9}$$

Where

$$A_{min} = \begin{bmatrix} -\frac{a_1 p + q}{a_2} & -\frac{p\left(4\omega^2 - a_1^2\right) - 2a_1 q}{4a_2\omega} \\ p & -\frac{a_1 p + 2q}{2\omega} \end{bmatrix}, \tag{10a}$$

$$B_{min} = x_r + \begin{bmatrix} \frac{a_1 p + q}{a_2} \\ -p \end{bmatrix}^T \quad , \tag{10b}$$

$$A_{max} = \begin{bmatrix} -\frac{a_1 v + z}{a_2} & -\frac{v\left(4\omega^2 - a_1^2\right) - 2a_1 z}{4a_2\omega} \\ v & -\frac{a_1 v + 2z}{2\omega} \end{bmatrix}, \tag{10c}$$

$$B_{max} = x_r + \begin{bmatrix} \frac{a_1 v + z}{a_2} \\ -v \end{bmatrix}^T \quad , \tag{10d}$$

$$X(t) = R(t)\cos(\omega t) \qquad Y(t) = R(t)\sin(\omega t) \tag{10e}$$

$$R(t) = e^{\frac{a_1}{2}t}\ , \tag{10f}$$

$$\begin{bmatrix} p & q \end{bmatrix}^T = Ax_r + Bu_{min}, \tag{10g}$$

$$\begin{bmatrix} v & z \end{bmatrix}^T = Ax_r + Bu_{max}, \tag{10h}$$

$$\omega = \frac{\sqrt{4a_2 - a_1^2}}{2} \tag{10i}$$

Applying the above mapping to the original state variables, we obtain (X, Y), from now on referred to as *normal variables* and the original state trajectory is turned into a logarithmic spiral.

By mapping the state trajectory, it is possible to generate the switching curves, which permit to calculate the number of switches; specifically, a switch in the control law occurs when the mapped state trajectory (black solid line in Figure 3) encounters these curves. In the normal coordinates, a switching curve is created by rotating the final state under u_{min} and u_{max} by π radians and scaling it by $e^{\frac{a_1\pi}{2\omega}}$. This process creates the three curves in Figure 3, where

- the first curve represents the trajectories reaching the final state under u_{max} (red line);
- the second curve indicates the trajectories reaching the final state under u_{min} (blue line);
- the third curve is called bounding curve because it divides the space into regions where the bang-bang control law has the same number of switches (green line).

The geometric parameters needed for the computation of the bang-bang control law are then:

- α, which represents the rotation to apply to the first switching curve, where it is crossed by the mapped state trajectory, in order to include p_0;
- β, which is the angle between the switching curve segment in the same region of p_0 and its centre of rotation;

Using α and β, it is possible to compute the switching times t_k, according to the following algorithm.

TIME-OPTIMAL CONTROL DESIGN

1) map the initial state x_0 according to M^-_{min} and M^-_{max}; the one that lies on the x-axis is called p_0 and is the initial state in the normal coordinates;
2) find the number of switches by searching in which regions p_0 lies;
3) the initial extreme of the bang-bang control law is

$$u(0) = \begin{cases} u_{min}, & if\ M^-_{min}\ was\ used \\ u_{max}, & if\ M^-_{max}\ was\ used \end{cases} . \tag{11}$$

4) calculate the switching times using the following formulas:
   - the time corresponding to the first switch is:

$$t_1 = \begin{cases} \frac{\pi+\alpha}{\omega}, & \alpha < 0, \\ \frac{\alpha}{\omega}, & \alpha \geq 0; \end{cases} \tag{12}$$

   - the intermediate switches times are:

$$t_k = t_1 + \frac{\pi}{\omega}(K-1)\ , \quad k = 2, 3, ..., K-1 \tag{13}$$

The following remarks are due.

Remark 1: Notice that, with the algorithm above defined, the total time for driving the system to the final condition can be easily computed and is equal to

$$T_s = t_1 + \frac{(K-1)\pi + \beta}{\omega}. \tag{14}$$

Remark 2: A second order system typically twists around its equilibrium point, which is different for every system. This method, using the map defined in (9), *standardizes* all

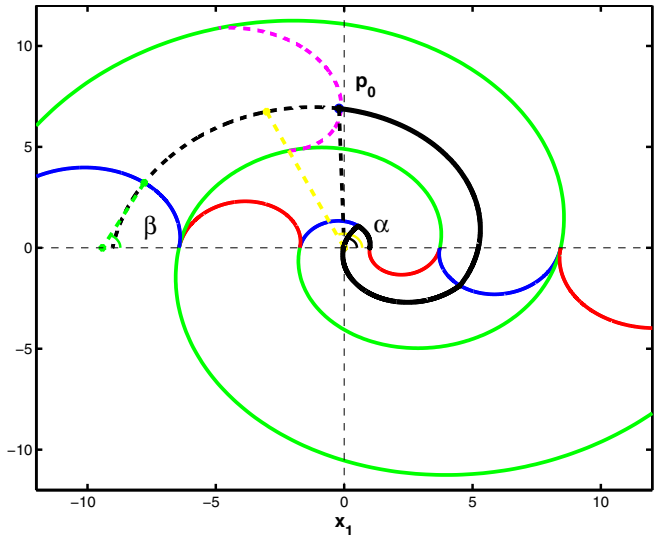

Fig. 3. Application of the geometric method for the computation of the bang-bang control law, using M^{-}_{min}. Switching curves (red and blue lines), bounding curves (green line) and trajectory of the state (black line). The point p_0 represents the initial conditions, whereas the target is denoted by $(1, 0)$.

the systems by placing the target always in $[1, 0]$ and transforming all the switching curves (which can be everywhere in the original state space), in semi-logarithmic spiral with centre of rotation placed on the x-axis.

Remark 3: Since the costate rotate at a fixed velocity ω (10i) and the maximum rotation between two switches is π radians (deduced from Equation (6)), the intermediate switch has a length of $\frac{\pi}{\omega}s$.

Remark 4: The duration of the first and the last switch depends on the *distance*, in degrees, from the switch limit. These *distances* are traduced in terms of α and β.

B. An approximation: proportional control

Once the benchmark performance in terms of time is known, a simpler controller can be designed, *e.g.* to meet the additional requirement of simplicity in the implementation. In this work, an approximation of the time-optimal controller will be proposed by employing a proportional controller acting on the bounded input speed.

Since the value of K_p can be easily calculated (to resemble to the time-optimal control scheme) without considering the saturation in the input, the internal stability will be guaranteed by an *a-posteriori* check. Such a verification method is based upon LMI-based analysis of anti-windup systems (see *e.g.* [3], [4], [2]) and can briefly described as follows.

To start with, consider the closed-loop dynamics obtained by inserting the proportional action

$$u = K_p y = Kx, \;\; K = [K_p, 0]^T$$

in the loop with (4).

Then, rewrite the system as fed by $q = u - \sigma(u)$. It can be shown [3], [4], [2] that the system turns out to be as

$$\begin{aligned} \dot{x} &= \bar{A}x + \bar{B}q \\ u &= Kx \\ q &= u - \sigma(u) \end{aligned} \tag{15}$$

where $\bar{A} = A + BK$ and $\bar{B} = -B$. Moreover, from the same reference, we know that proving internal stability is equivalent to show the feasibility of the LMI problem

$$P = P^T > 0, \; W \geq 0 \text{ diagonal}, \tag{16}$$

$$\begin{bmatrix} \bar{A}^T P + P\bar{A} & P\bar{B} + K^T W \\ B^T P\bar{B} + W^T K & -2W \end{bmatrix} < 0, \tag{17}$$

for at least one choice of matrices P and W, such that (16) holds. Notice that, once the stability verification is done, the proportional controller can be used in the same experimental conditions of the time-optimal one.

The time suboptimal control design procedure can then be summarized as follows.

TIME-SUBOPTIMAL CONTROL DESIGN

- design the time-optimal controller in the nominal case;
- tune a proportional controller, which resembles to the time-optimal one in the nominal case;
- check the stability of closed-loop system with the proportional controller and saturated input, by verifying the feasibility of (16) and (17)
- implement the proportional controller on the real system.

In the next section, we will show that such an approximation will provide (slightly) worse performance in the nominal case but it will be more robust in case of parametric uncertainties.

IV. Simulation Results

In order to evaluate the performance of the considered strategies, both the introduced controllers - the time-optimal one and its approximation using a single gain - are now simulated under the same conditions.

The bridge crane system considered in the next examples is (4), where the physical parameters are selected as follows.

$$m = 1000 \; Kg, \;\; r = 5 \; m, \;\; g = 9.81 \; m/s^2, \;\; b = 12000$$

Concerning the bounds on the motor current, the input is assumed to belong to $[-10, 10]$.

As already mentioned, the payload reaches the maximum oscillation angle when the sway speed is equal to zero. Generally, 10 degrees of oscillation represent a dangerous condition, thus motivating the use of a controller which quickly moves and stops the load. Then, we select the initial conditions of the experiments as

$$x_0 = \begin{bmatrix} \theta \\ \dot{\theta} \end{bmatrix} = \begin{bmatrix} 10 \\ 0 \end{bmatrix}. \tag{18}$$

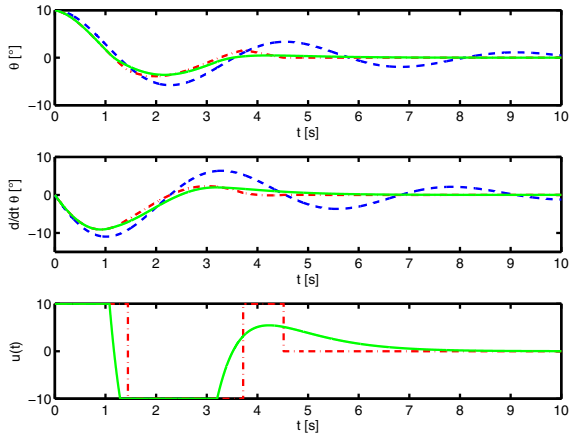

Fig. 4. Simulation results: response of the system without control (dashed line); response with the proportional controller (solid line) and response with the time-optimal controller (dash-dotted line).

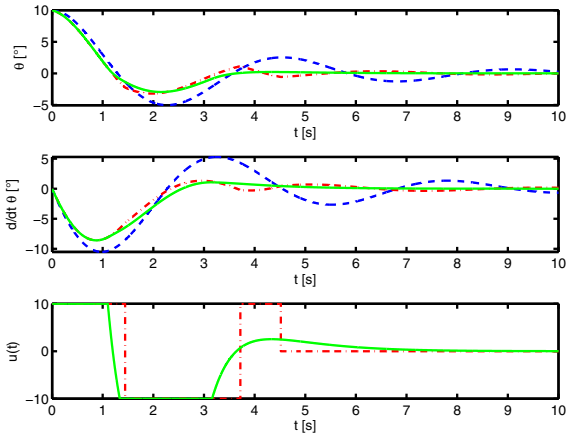

Fig. 5. Simulation results with no control (dashed line), with time-optimal control (dash-dotted line) and with proportional control (solid line). In the experiments, the mass is decreased of 5%, the length of the rope of 2% and the friction coefficient is increased of 15% with respect to the nominal values.

The final condition is instead given by

$$x_r = \begin{bmatrix} \theta \\ \dot{\theta} \end{bmatrix} = \begin{bmatrix} 0 \\ 0 \end{bmatrix}. \tag{19}$$

In Figure 4, the results of the simulation under the conditions described above are illustrated. Without control (blue line), the system shows the response of a second order system with conjugate poles and low damping. Using the proportional controller (green line), the oscillations are instead significantly reduced. Notice that the time-optimal controller takes the least time possible and therefore it is the best in terms of settling time. In Table I, the quantitative performance of the controller in terms of maximum overshoot and settling time are briefly summarized. It should be noticed

	Settling Time [s]	Max Overshoot [%]
Without Control	> 15	57.9
Time-Optimal Control	4.47	39.1
P Control	6.31	36.2

TABLE I

PERFORMANCE OF TIME-OPTIMAL AND PROPORTIONAL CONTROLLER IN THE NOMINAL CASE.

that, although the time-optimal controller ensures quickly damping of the oscillations, the maximum sway angle is bigger than the one given by the proportional controller. This is indeed reasonable, as the bang bang control law exploits the most of the control power to stop the system, and this is generally converted into quite aggressive control requirements.

A. Robustness issue

The model described in section II is generally a good approximation of the reality. However, the three physical parameters can in practice be subject to some uncertainties, *e.g.*,

- concerning the payload: its weight cannot be known exactly, as standard bridge cranes do not have a load cell to estimate the mass of the cargoes.
- concerning the length of the rope: this information is sometimes available and easily obtainable using an encoder. However, some uncertainty may come from the connection of the payload to the rope; as a matter of fact, the cargoes are often connected to the hook using a cable, thus leading to an error in the estimation of r.
- concerning the friction coefficient: this parameter is the least accurate since it is strongly dependent on the environmental conditions (see *e.g.* [9], [1]) and it is hard to measure on-line.

Due to the above considerations, we test the robustness of the two controllers in case of undesired parametric variations. More specifically, as an example, we consider the realistic case where:

- the payload mass has an error of -5%;
- the rope length has an error of -2%;
- the friction coefficient has an error of 15%.

In Figure 5, the results of the simulations on the system with parametric variations are illustrated. In the experiments, we used the same control laws of the last section (*i.e.*, considering the nominal model).

As shown in Table II, the performance of the time-optimal controller significantly jeopardizes, due to the variations in the parameters of the model. In particular, the settling time, which was the strength of the time-optimal strategy, is now about $4s$ slower than P control. On the other side, the maximum overshoot maintains the same behaviour, whereas the proportional controller reduces the maximum oscillation angle and it is now better than the time-optimal solution. The loss of performance of the time-optimal control is due to the variation in the model, which makes the bang-bang control strategy switch at wrong times. This behaviour is evident in

	Settling Time [s]	Max Overshoot [%]
Time-Optimal Control	9.38	32
P Control	5.66	29.5

TABLE II

PERFORMANCE OF TIME-OPTIMAL AND PROPORTIONAL CONTROLLER IN CASE OF PARAMETRIC VARIATIONS.

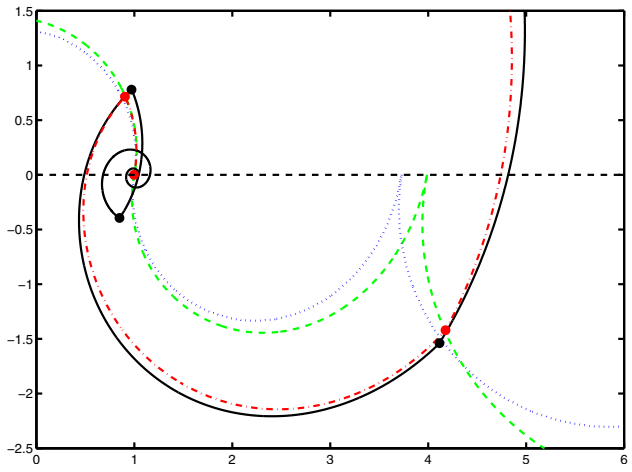

Fig. 6. The figure show the loss of optimality applying the bang-bang law to system with parameters different from the nominal ones. Switching curves for the system without (dotted line) and with uncertainties (dashed line); state trajectory with the correct bang-bang law (dash-dotted line) and with a wrong one (solid line).

Figure 6, where:

- the green and blue line represent the switching curves for the system with and without parametric uncertainties respectively;
- the red line is the system response under the bang-bang control law based on the system with the new correct values of the parameters;
- the black line is the system response under the bang-bang control law based on the nominal system.
- the points (in red and black) denote the switching times.

As expected, there is an error in the switching times; in fact, the black line does not switch when the switching curve is crossed. This fact obviously leads to the loss of the optimality of the time-optimal controller.

Based on the above results, we could then conclude that, in some real-world situations, the most promising approach for time-optimal control - *in practice* - turns out to be the suboptimal procedure at the end of Section III.

V. CONCLUSIONS

In this paper, the problem of damping the residual load swinging when the bridge crane stops has been dealt with. More specifically, the problem of minimizing the time to stop the crane has been considered. From this perspective, it has been shown that the bridge crane perfectly fits the theoretical framework of the recently introduced technique in [12], which allows the control designer to devise a bang bang control law without the need of computing the analytical trajectory of the costate. This technique has been shown to perform very well in a simulation example. However, since in bridge cranes the mass of the payload as well as the damping coefficient and other parameters may be subject to several uncertainties, this technique has been shown to be no longer suitable in some practical situations. Nonetheless, a proportional controller - which can be tuned to resemble to the time-optimal one in the nominal case - can be implemented on the real system to provide a larger robustness margin. Such a controller is also easier to implement and can be guaranteed to stabilize the system even in presence of saturation of the motor current using LMI conditions.

Future work will be devoted to the experimental assessment of the two design methods on a real bridge crane.

REFERENCES

[1] C Canudas de Wit. Robust control for servo-mechanisms under inexact friction compensation. *Automatica*, 29(3):757–761, 1993.

[2] Sergio Galeani, M Massimetti, Andrew R Teel, and Luca Zaccarian. Reduced order linear anti-windup augmentation for stable linear systems. *International journal of systems science*, 37(2):115–127, 2006.

[3] Gene Grimm, Jay Hatfield, Ian Postlethwaite, Andrew R Teel, Matthew C Turner, and Luca Zaccarian. Antiwindup for stable linear systems with input saturation: an lmi-based synthesis. *Automatic Control, IEEE Transactions on*, 48(9):1509–1525, 2003.

[4] Gene Grimm, Andrew R Teel, and Luca Zaccarian. Linear lmi-based external anti-windup augmentation for stable linear systems. *Automatica*, 40(11):1987–1996, 2004.

[5] Y. Liang H. Lee and D. Segura. A new approach for the antiswing control of overhead cranes with high-speed load hoisting. *Int. J. Control,*, 76(15):1493–1499, 2003.

[6] Huey J. Singhose W. Khalid A., Frakes D. and Lawrence J. Human operator performance testing using an input-shaped bridge crane. *Journal of dynamic systems, measurement, and control*, 128:835–841, 2006.

[7] Joseph Pierre LaSalle. The time optimal control problem. *Contributions to the theory of nonlinear oscillations*, 5:1–24, 1960.

[8] Raymond Manning, Jeffrey Clement, Dooroo Kim, and William Singhose. Dynamics and control of bridge cranes transporting distributed-mass payloads. *Journal of dynamic systems, measurement, and control*, 132(1), 2010.

[9] Lrinc Marton and Bla Lantos. Modeling, identification, and compensation of stick-slip friction. *Industrial Electronics, IEEE Transactions on*, 54(1):511–521, 2007.

[10] A Piazzi and A Visioli. Optimal dynamic-inversion-based control of an overhead crane. *IEE Proceedings-Control Theory and Applications*, 149(5):405–411, 2002.

[11] Lev Semenovich Pontryagin, VG Boltyanskii, RV Gamkrelidze, and EF Mishchenko. The mathematical theory of optimal processes. 1962.

[12] Zhaolong Shen, Peng Huang, and Sean B Andersson. Calculating switching times for the time-optimal control of single-input, single-output second-order systems. *Automatica*, 2013.

[13] William Singhose, Dooroo Kim, and Michael Kenison. Input shaping control of double-pendulum bridge crane oscillations. *Journal of Dynamic Systems, Measurement, and Control*, 130(3), 2008.

[14] Joshua Vaughan and William Singhose. Input shapers for reducing overshoot in human-operated flexible systems. In *American Control Conference, 2009. ACC'09.*, pages 178–183. IEEE, 2009.

[15] Gao Jiyong Lai Xinming and Wang Jinnuo. Dynamic analysis and optimization of a bridge crane. *Journal of Machine Design*, 6:004, 1994.